CHEMMEDCHEM

DOI: 10.1002/cmdc.201000109

Novel Peptidyl Aryl Vinyl Sulfones as Highly Potent and Selective Inhibitors of Cathepsins L and B

Laura Mendieta,[a] Anna Picó,[b] Teresa Tarragó,[a] Meritxell Teixidó,[a] Marcos Castillo,[b] Llorenç Rafecas,[c] Albert Moyano,*[b] and Ernest Giralt*[a, b]

Herein we present the design, synthesis, and evaluation of a structurally novel library of 20 peptidyl 3-aryl vinyl sulfones as inhibitors of cathepsins L and B. The building blocks, described here for the first time, were synthesized in a highly efficient and enantioselective manner, starting from 3-aryl-substituted allyl alcohols. The corresponding vinyl sulfones were prepared by a new approach, based on a combination of solid-phase peptide synthesis using the Fmoc/*t*Bu strategy, followed by solution-phase coupling to the corresponding (*R*)-3-amino-3-aryl vinyl sulfones as trifluoroacetate salts. The inhibitory activity of the resulting compounds against cathepsins L and B was evaluated, and the compound exhibiting the best activity was selected for enzymatic characterization. Finally, docking studies were performed in order to identify key structural features of the aryl substituent.

Introduction

Cathepsins constitute a widespread group of proteases, a majority of which belong to the C1 family of the cysteine protease clan CA (CAC1).[1,2] Cathepsins are implicated in a variety of processes, including protein turnover, enzyme activation, hormone maturation, bone resorption, antigen presentation and epidermal homeostasis.[2,3,4] On the basis of sequence similarity, CAC1 cysteine proteases are divided into two groups: cathepsin L-like (which includes mammalian cathepsins L, K, and S, protozoan falcipains, rhodesain, cruzain, and CPA and CPB *Leishmania* proteases), and cathepsin B-like (including cathepsin B and the CPC *Leishmania* proteases).[2]

In healthy cells, cathepsins are localized in lysosomes.[2,4,5] Initially, they were thought to be housekeeping enzymes, but they are now recognized to have other functions in healthy cells: they process proteins in the nucleus and intracellular organelles, such as hormone secretory granules, and play specific roles in physiological processes, such as bone remodeling, and epidermal homeostasis.[6] Furthermore, they are highly regulated at several stages of the cell cycle, and their expression levels vary depending on the tissue.[5]

Cathepsins also play a key role in a number of human diseases, such as rheumatoid arthritis and cancer. In cancer cells, as well as in cytotoxic T lymphocytes and natural killer cells, cathepsins are rerouted from lysosomes to the cell surface.[6] In some types of cancer, cathepsins are also secreted to the exterior.[6,7,8] Because the extracellular microenvironment of tumors is generally acidic, cathepsins are still able to cleave other peptides and proteins following translocation.[6] They also degrade the basement and the extracellular matrix,[6,7,8] thereby promoting angiogenesis and invasive tumor growth[7] and metastasis.[7,8] The expression and activity of cathepsins are also modified in cancer cells. There is a progressive increase in cathepsin levels during tumorigenesis,[7,8] which correlates with a higher malignancy of the tumor.[6,7,8] The activity is localized and clearly evident in angiogenic islets and tumors, particularly on the edges of the islet carcinomas.[7]

Cathepsin B degrades three of the most important basement components,[7,9] resulting in proteolysis of surrounding tissues and allowing cancer cell invasion.[10] Treatment of in vitro human cancer cells[10] and of in vivo mice tumors with cathepsin inhibitors decreases the volume,[7] invasion[6] and growth of tumors.[7,11] These data were confirmed by knockdown experiments, with a decrease in cell proliferation observed in tumors from cathepsin B (44% decrease) and cathepsin L (58%) knockout mice.[11] Furthermore, a decrease in vessel density of tumors has been reported in response to treatment with cathepsin B and L inhibitors.[7] Additionally, selective inhibition of the tumor-promoting cathepsins results in a decrease in tumor invasiveness.[12]

The inhibition of cathepsins L and B has, therefore, recently gained interest as a key strategy for the development of new anticancer drugs. To date, many reversible and irreversible cathepsin L and B inhibitors have been described. With respect to reversible inhibitors, the reactive group can be an alde-

[a] *L. Mendieta, Dr. T. Tarragó, Dr. M. Teixidó, Prof. Dr. E. Giralt*
Institute for Research in Biomedicine of Barcelona
Barcelona Science Park, Baldiri Reixac 10, 08028 Barcelona (Spain)
Fax: (+34) 934037126
E-mail: ernest.giralt@irbbarcelona.org

[b] *Dr. A. Picó, Dr. M. Castillo, Prof. Dr. A. Moyano, Prof. Dr. E. Giralt*
Departament de Química Orgànica, Universitat de Barcelona
Martí Franquès, 1-11, 08028 Barcelona (Spain)
Fax: (+34) 933397878
E-mail: amoyano@ub.edu

[c] *L. Rafecas*
ENANTIA S.L.
Barcelona Science Park, Baldiri Reixac 10, 08028 Barcelona (Spain)

Supporting information for this article is available on the WWW under http://dx.doi.org/10.1002/cmdc.201000109.

hyde,[13] an aldehyde-hydroxamic acid combination,[14] nonpeptidic cyanamide,[15] dipeptidyl nitrile[16] or β-lactam penam or oxapenam compounds.[2] All of these are selective cathepsin L inhibitors, except the dipeptidyl nitriles, which show higher affinity for cathepsin B. Irreversible inhibitors include E-64 analogues[2] (mainly cathepsin B and L inhibitors) and alkyl vinyl sulfones (cathepsin B, L, O2, and S inhibitors).[17,18,19] Peptidyl vinyl sulfones comprise a group of potent, selective and covalent inhibitors of cysteine proteases, with proven efficacy against other cysteine proteases, such as cruzipain[2,20,21] and cathepsins S,[22] K,[23] and F.[24]

4-morpholinylcarbonyl-L-leucine-(1*S*)-(2-phenylethyl)-3-(phenylsulfonyl)-(2*E*)-propenamide (Figure 1 A), a peptidyl 3-alkyl vinyl sulfone derived from the cathepsin S inhibitor homophenylalanine, has been identified as an antimalarial compound.[17] Unfortunately, it was a potent but nonselective inhibitor.[17,25] Compound *N*-(4-morpholinylcarbonyl)-L-phenylalanine-(1*S*)-(2-phenylethyl)-3-(phenylsulfonyl)-(2*E*)-propenyl amide (Figure 1 B) was designed in a collaboration between pharmaceutical companies.[25] Further modification of these original compounds led to *N*-(4-methylpiperazin-1-ylcarbonyl)-L-phenylalanine-(1*S*)-(2-phenylethyl)-3-(phenylsulfonyl)-(2*E*)-propenyl amide (Figure 1 C), a potent cruzipain inhibitor[20] that is now under active development as an anti-trypanosomal therapeutic compound.

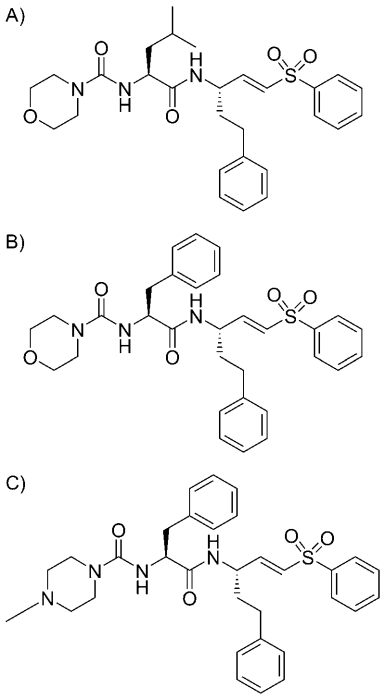

Figure 1. Peptidyl vinyl sulfones previously described as cysteine protease inhibitors.

The most common strategy for the preparation of peptidyl vinyl sulfones relies on conventional methods of peptide synthesis whereby the corresponding 3-amino vinyl sulfone is coupled with amino acids or peptide derivatives. However, there are very few methods available for the synthesis of enantiomerically pure 3-amino vinyl sulfones, all of which use α-amino acids as starting materials and generally follow a synthetic route that requires their reduction to α-amino aldehydes and a subsequent Wadsworth–Emmons reaction with a sulfonylmethyl phosphonate.[18] This imposes strong limitations on the structural variability of the corresponding peptidyl vinyl sulfone derivatives. In particular, no aryl vinyl sulfone compounds have been described in the literature as cathepsin inhibitors, likely due to the easy racemization of the intermediate α-amino-α-aryl aldehydes. Based on a general route to *N*-Boc-3-amino vinyl sulfones previously developed in our laboratories,[26] we herein report the synthesis of a structurally novel library of peptidyl 3-aryl vinyl sulfones as inhibitors of cathepsins L and B. These compounds were prepared by a novel method using an Fmoc/*t*Bu solid-phase synthesis strategy, followed by solution-phase coupling to the corresponding 3-amino-3-aryl vinyl sulfones. The inhibitory activities of these compounds against cathepsins L and B were evaluated.

Results and Discussion

Library design and synthesis

The designed library was based on the scaffold presented in Figure 2, in which X is either oxygen (making position 1 a morpholinyl group) or an *N*-methyl group (resulting in a 4-methylpiperazinyl group in position 1). R^2 can be either isobutyl (so that the amino acid in position 2 is Leu) or benzyl (yielding the amino acid Phe in position 2). The highest variability was introduced at the R^1 position with five different groups: phenyl, 1-naphthyl, 2-naphthyl, mesityl (2,4,6-trimethylphenyl), and 4′-biphenyl, thereby enabling for the first time a systematic evaluation of structure–activity relationships with respect to aryl chain substituents in position 1 of the peptidyl vinyl sulfone. The combination of all of the substituents in the scaffold gave rise to 20 distinct structures for our library. It is worth noting here that the structural diversity of this library can be easily increased by sulfone substituent variations, which we restricted to an unsubstituted phenyl group. To maintain the same chirality as known inhibitors, the absolute configuration of the two stereogenic centers of this scaffold was *S* for the amino acid in position 2 and *R* for the 3-amino-3-aryl vinyl sulfone.

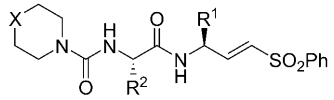

Figure 2. Proposed library of peptidyl 3-aryl vinyl sulfones.

The peptidyl 3-aryl vinyl sulfones were synthesized in a three-step strategy: coupling of the position 2 amino acid to the resin, construction of the morpholineurea (Mu) or 4-methylpiperazineurea (Npipu) group, and solution-phase coupling

to 3-amino-3-aryl vinyl sulfones. The first two steps were done in solid phase; the main advantage of this methodology is that reactions can be driven to completion by use of excess reagents. Purification is performed after each step by simply washing away the excess reagents. In contrast, more intensive purification and characterization are required after each step in solution-phase syntheses. In the synthesis of the peptidyl 3-aryl vinyl sulfones, using the solid-phase method also enables the preparation of a large quantity of the urea amino acid unit that can later be divided for reactions with the various sulfones in solution. The key *N*-Boc-(*R*)-3-amino-3-aryl vinyl sulfones **1**–**5** were prepared with good overall yields, complete diastereoselectivity (*E* configuration of the double bond), and excellent enantiomeric purities (>95:5 er) using the synthetic sequence outlined in Scheme 1. This sequence began with readily available (*E*)-3-aryl-2-propenols and relied on the Sharpless catalytic epoxidation with D-(−)-diisopropyl tartrate as the chiral ligand for the establishment of the absolute *R* configuration of the final compounds.[26] Prior to the coupling step, *N*-Boc-(*R*)-3-amino-3-aryl vinyl sulfones **1**–**5** were treated with a solution of trifluoroacetic acid (TFA, 40% in dichloromethane) to afford the corresponding trifluoroacetate salts **6**–**10**.

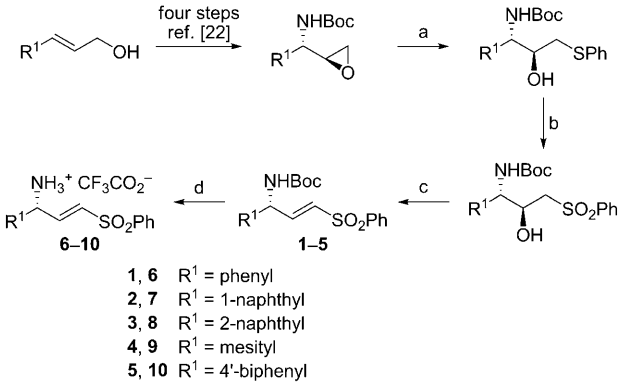

Scheme 1. *Reagents and conditions*: a) PhSH, Et_3N, CH_2Cl_2, CH_3OH, reflux; b) *m*-CPBA, CH_2Cl_2, RT (61–88% yield, two steps); c) morpho-CDI, cat. $CuCl_2$, CH_3CN, RT (90–100% yield); d) 40% TFA in CH_2Cl_2, RT (quant).

For solid-phase synthesis of the urea–amino acid moieties, we used a 2-chlorotrityl resin, following the Fmoc/*t*Bu strategy (0.7 equiv of Fmoc-aa-OH, 7 equiv *N*,*N*-diisopropylethylamine (DiPEA) in dichloromethane, room temperature; capped with methanol, 20% piperidine in *N*,*N*-dimethylformamide (DMF), room temperature) to introduce the amino acid. The coupling yields for Phe and Leu were 82 and 83%, respectively. The Fmoc group was removed with 20% piperidine in DMF. Condensation with 4-morpholinocarbonyl chloride in the presence of DiPEA in DMF, followed by cleavage from the resin with 2% TFA in dichloromethane, yielded the corresponding morpholine-derived ureas. Purification by preparative HPLC afforded the desired compounds Mu-Phe-OH and Mu-Leu-OH, in 70 and 76% yield, respectively. However, this protocol (using *N*-methylpiperazinocarbonyl chloride) was not suitable for the synthesis of the *N*-methylpiperazine-derived ureas. Instead, these syntheses were ultimately accomplished by reaction of the resin-bound amino acid with carbonyl diimidazole in DMF, followed by treatment with a large excess (20 equiv) of *N*-methylpiperazine. After cleavage and purification, the target urea–amino acid conjugates Npipu-Phe-OH and Npipu-Leu-OH were isolated in 100 and 55% yield, respectively. The final solution-phase coupling was carried out by reaction of the urea–amino acid fragments with the (*R*)-3-amino-3-aryl vinyl sulfone trifluoroacetate salts in the presence of DiPEA, using either PyBOP/HOAt (method A) or *N*-cyclohexylcarbodiimide *N*′-methyl polystyrene HL (method B) in dichloromethane. The resulting peptidyl aryl vinyl sulfones **11**–**30** were purified by preparative HPLC (Scheme 2 and Table 1).

Biological activity

The inhibitory activity of the library against cathepsins L and B was evaluated. All inhibitors were analyzed fluorimetrically using the human enzymes as well as substrate Z-Phe-Arg-AMC for cathepsin L and Z-Arg-Arg-AMC for cathepsin B. The concentrations required for half-maximal inhibition (IC_{50}) were calculated as an initial screening assay and used to select the most promising compounds.

All compounds exhibited greater inhibitory capacity toward cathepsin L than cathepsin B (Table 2). The cathepsin inhibitory efficacy of aryl vinyl sulfones, with regard to substituents, was also determined. In general, compounds with a 4-methylpiperazinyl group in position 1 were more active than compounds with a morpholinyl group. In position 2, Phe yielded better

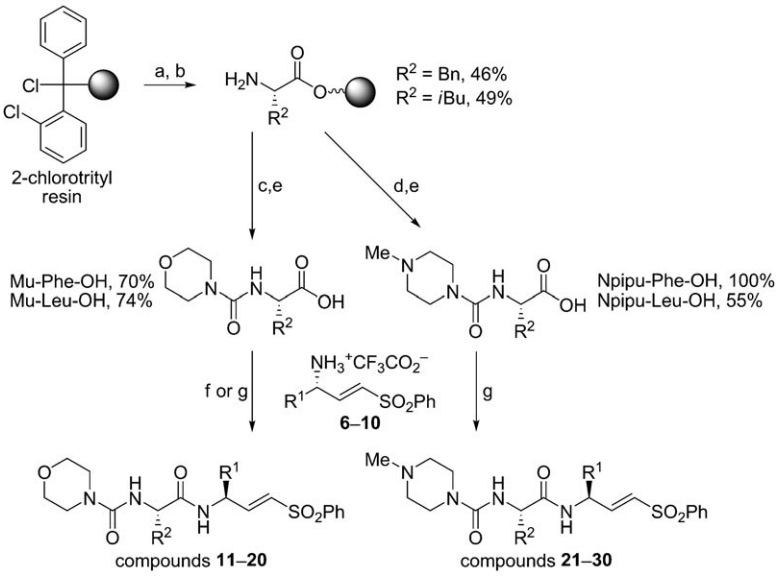

Scheme 2. *Reagents and conditions*: a) Fmoc-aa-OH (0.7 equiv), DiPEA (1 equiv), CH_2Cl_2, RT; b) 20% piperidine in DMF, RT; c) 4-morpholinocarbonyl chloride (1 equiv), DiPEA (2 equiv), DMF, RT; d) carbonyl diimidazole (5 equiv), *N*-methylpiperazine (20 equiv), DMF, RT; e) 2% TFA in CH_2Cl_2, RT; f) method A: PyBOP (1.1 equiv), HOAt (2.1 equiv), DiPEA (2.1 equiv), CH_2Cl_2, RT; g) method B: *N*′-methylpolystyrene HL (3 equiv), DiPEA (2.1 equiv), CH_2Cl_2, RT.

Table 1. Structures and yields for solution-phase coupling and purification of the library compounds.

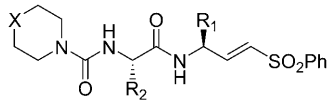

Compd	X	R^1	R^2	Method[a]	Yield [%][b]
11	O	Phenyl	Bn	A	78
12	O	1-Naphthyl	Bn	A	10
13	O	2-Naphthyl	Bn	A	6
14	O	Mesityl	Bn	A	18
15	O	4′-Biphenyl	Bn	B	44
16	O	Phenyl	*i*Bu	A	56
17	O	1-Naphthyl	*i*Bu	A	28
18	O	2-Naphthyl	*i*Bu	A	16
19	O	Mesityl	*i*Bu	A	30
20	O	4′-Biphenyl	*i*Bu	B	43
21	NMe	Phenyl	Bn	B	26
22	NMe	1-Naphthyl	Bn	B	33
23	NMe	2-Naphthyl	Bn	B	61
24	NMe	Mesityl	Bn	B	29
25	NMe	4′-Biphenyl	Bn	B	38
26	NMe	Phenyl	*i*Bu	B	28
27	NMe	1-Naphthyl	*i*Bu	B	81
28	NMe	2-Naphthyl	*i*Bu	B	57
29	NMe	Mesityl	*i*Bu	B	46
30	NMe	4′-Biphenyl	*i*Bu	B	51

[a] Method A: PyBOP as coupling agent; method B: *N*′-methyl polystyrene HL as coupling agent. [b] Yield of coupling step after purification by preparative HPLC.

results than Leu for cathepsin B, while cathepsin L did not discriminate between these two residues. Finally, in position 3, phenyl group compounds were preferred for cathepsin L while 2-napthyl compounds exhibited higher potency for cathepsin B. Compound **30** was not only the strongest inhibitor of cathepsin L (IC_{50} = 2.6 nM), but it also presented the highest selectivity toward this protease ($IC_{50\ CatB}/IC_{50\ CatL}$ = 404). Compound **28** was also a potent inhibitor of cathepsin L (IC_{50} = 4.9 nM). The inhibitor with highest activity toward cathepsin B was compound **23**, although this compound did not demonstrate selectivity (IC_{50} = 304 nM; $IC_{50\ CatB}/IC_{50\ CatL}$ = 17). As a control, IC_{50} values of E-64 were calculated for cathepsins L (IC_{50} = 8.3 nM) and B (IC_{50} = 2.3 nM).

Selectivity of peptidyl aryl vinyl sulfones for the cathepsins was evaluated against serine proteases prolyl oligopeptidase (POP) and dipeptidyl peptidase IV (DPP IV). Compounds **23** and **30** were tested at 100 and 500 μM, with no significant inhibition observed for DPP IV. In the case of POP, the IC_{50} values were higher than 100 μM. (Supporting Information table 1).

Elucidation of the inhibition mechanism

Time-course experiments of compound **30** against cathepsin L were carried out to study the mode of inhibition and characterize the kinetic parameters. The representation of enzyme activity versus time confirmed that aryl peptidyl vinyl sulfone **30** was a time-dependent inhibitor (Figure 3). Compound 30 was

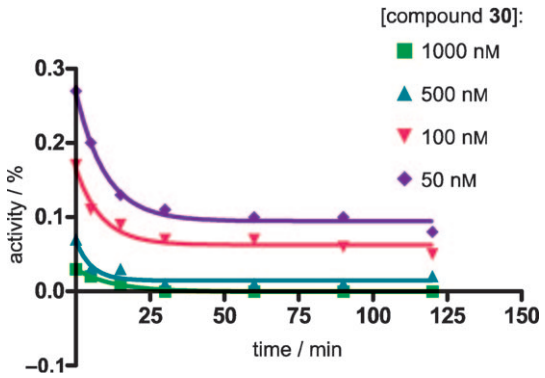

Figure 3. Time-course experiment of compound **30** against cathepsin L.

therefore defined as an irreversible inhibitor of cathepsin L with a second-order rate constant (k_2) of 181.420 $s^{-1}\,M^{-1}$. Kinetic experiments for compounds **30** (against cathepsin L) and **23** (against cathepsin B) were performed in order to further study the inhibitory mechanisms of action; Lineweaver–Burk plots (Supporting Information figure 1) showed competitive inhibition of the respective proteases.

With regard to the interaction between inhibitors and proteins, peptidyl aryl vinyl sulfones are well established covalent inhibitors of cysteine proteases. As such, they undergo a Michael addition with the thiol group of the active site cysteine to form an irreversible thioether bond.[17,18,19,27,28] This is also our mechanistic hypothesis for the compounds described herein.

Docking

To provide a structural basis for the data with our new peptidyl aryl vinyl sulfones, we performed computational docking studies. Compounds **30** and **29** were docked to human cathepsin L (PDB ID: 1CS8) and compound **23** to human cathepsin B (PDB ID: 1HUC).[29] No covalent binding was considered in the docking studies. The protein was set as rigid; therefore, reported distances may be smaller due to its flexibility as potential hydrogen bonds may be favored following first approach and contact of the compound with the protein.

Docking of compound **30** in the cathepsin L active site showed that the inhibitor extended from S2 to S2′ (Figure 4). Aryl vinyl sulfone **30** interacts with active site Cys25 through two potential hydrogen bonds, one with the oxygen atom of position 2 and one with the oxygen atom of the sulfone group (Figure 5 A). Cys25 is also adjacent to the β-vinyl carbon; this proximity may favor nucleophilic attack of the sulfur atom and subsequent formation of a covalent bond (Figure 5 B). Compound **30** also interacts with active site His163 through a hydrogen bond (Figure 5 C), while two other hydrogen bonds might be formed after the inhibitor approaches the protein.

The sulfone, located near S2, is one of the groups that appears to interact most strongly with cathepsin, through two hydrogen bonds and three more potential bonds involving Cys25, Trp26, and Gly68 (Supporting Information figure 2). The 4′-biphenyl substituent is surrounded by Asn66 and Gln21 (Fig-

Table 2. Inhibition of cathepsins L and B by the library of peptidyl 3-aryl vinyl sulfones.

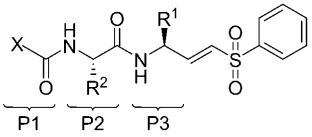

Compd	Substituents X	Substituents R^2	Substituents R^1	IC_{50} [nM] Cathepsin L	IC_{50} [nM] Cathepsin B
11			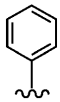	32	865
12			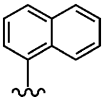	$>10^5$	$>10^5$
13			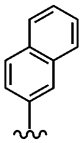	1000–1500	860
14			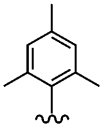	$>10^5$	$>10^5$
15			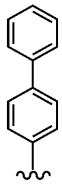	100–1000	415
16			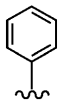	860	1700
17			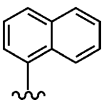	5×10^6	$>10^5$
18			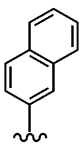	10	703
19			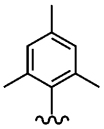	10^5	$>10^5$
20			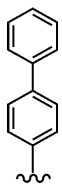	930	660

ure 5D). Other hydrogen bonds may be possible in the interaction between compound **30** and cathepsin L, involving residues Asp162, Gln19 and Trp189, which may form favorable contacts between these molecules. Finally, the 4-methylpiperazinyl group, located near S2′, may form three hydrogen bonds with residues Gln19 and Cys22 (Supporting Information figure 3).

To further understand the differences in inhibition rates, compound **29** was docked against cathepsin L. Compound **29** differs from compound **30** only at position 2 (mesityl group versus 4′-biphenyl, respectively). In spite of this single change, the effectiveness of the inhibitor decreases 500-fold. This can be attributed to the large volume occupied by the mesityl group, in comparison with the 4′-biphenyl group. The bulkiness of the mesityl group prevents it from fitting into subsite S1, the area delineated by Asn66 and Gln21, whereas compound **30** fits very well into this same site. As a result, the backbone of compound **29** cannot be accommodated near the cathepsin surface, increasing the distances of potential hydrogen bonds and decreasing the binding energy (Supporting Information figure 4).

The catalytic residues of cathepsin B include Cys29, His199, and Asn219. Compound **23** demonstrates the capacity to form hydrogen bonds with His199 (Figure 6B) and Cys29 (Supporting Information figure 5). The sulfone group of compound **23** is likely to form a total of five hydrogen bonds with Gly27, Cys29, His199, and Ala200 (Supporting Information figure 6) while the 2-naphthyl group is surrounded by His111, Val176, Leu181, and Met196 (Figure 6C). Finally, the 4-methylpiperazinyl group forms one hydrogen bond and has three

Table 2. (Continued)

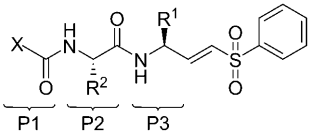

Compd	Substituents X	Substituents R^2	Substituents R^1	IC_{50} [nM] Cathepsin L	IC_{50} [nM] Cathepsin B
21			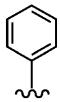	100	520
22			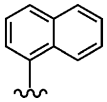	5×10^4	5×10^4–10^5
23			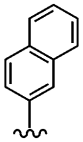	17.5	304
24			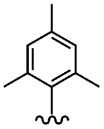	$>10^5$	$>10^5$
25	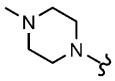		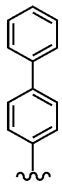	8.5	300
26			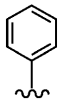	82	886
27			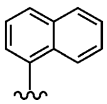	536	$>10^5$
28			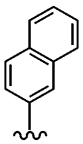	5	690
29			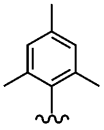	>1000	$>10^5$
30			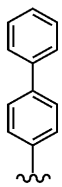	2.6	1050

other potential ones with residues His110, His111, and Trp221 (Supporting Information figure 7).

Conclusions

For the first time, we have applied a new methodology that combines solid-phase and solution syntheses for the production of a structurally novel peptidyl 3-aryl vinyl sulfone library. We screened the library and identified powerful inhibitors of cathepsins L and B. The most active compound was further studied and determined to be an irreversible covalent competitive inhibitor. Finally, docking studies were performed, with analysis of the results corroborating the experimental data. Because cathepsins L and B are currently key targets for the treatment of cancer, the inhibitors described herein constitute interesting and promising candidates for the development of new anticancer drugs.

Experimental Section

Materials and methods

Melting points were determined in an open capillary tube by means of a Gallenkamp apparatus and were not corrected. Specific rotations were determined at room temperature (25 °C) in a PerkinElmer 241 MC instrument; concentrations are given in g(100 mL)$^{-1}$. NMR spectra (^{1}H, ^{13}C) were recorded using a Varian-Gemini 200 (^{1}H 200 MHz) or a Mercury 400 instrument (^{1}H 400 MHz). Signal multiplicity in ^{13}C NMR spectra was established by means of DEPT or HSQC experiments. Mass spectra using CI, ESI, or FAB techniques were recorded on a Hewlett–Packard HP-5988A instrument. MALDI-TOF spectra, using an ACH (α-cyano-4-hydroxycinnamic acid) matrix, were determined in a Voyager-DE RP instrument (PE Biosystems) with a 337 nm nitrogen laser. Analytical HPLC was performed using a Waters 1525 instru-

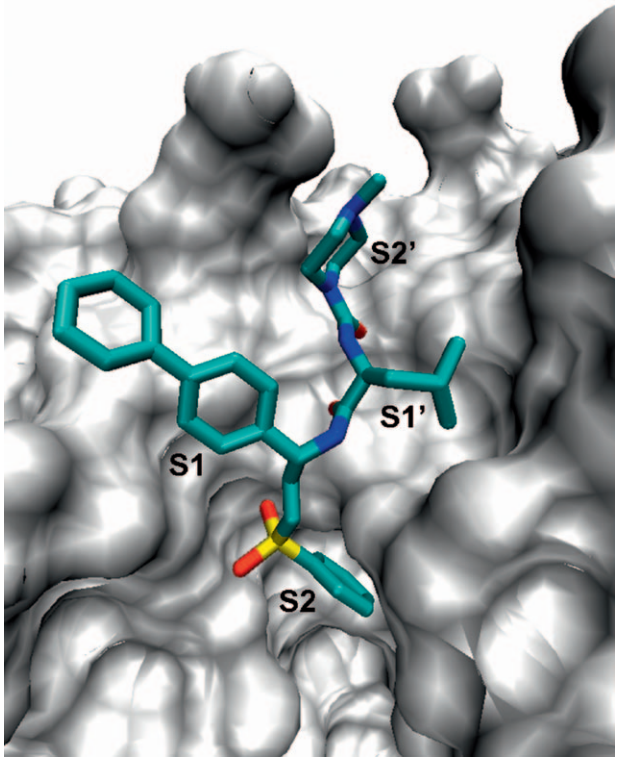

Figure 4. Docking of compound **30** in cathepsin L subsites. C atoms are shown in light green; N, O, and S atoms are colored by atom type.

ment (photodiode array Waters 996 detection) or in a Waters Alliance 2795 instrument (MS-ESP ZQ detection). Preparative HPLC purifications were performed with a Waters 600 instrument, using automatic injection (Waters 2700), UV/Vis two-channel detection (Waters 2847), and automatic fraction collection (Waters Fraction Collector II), with a Symmetry C_{18} (100×30 mm) column.

Solvents (DMF, CH_2Cl_2, CH_3CN, $CHCl_3$, CH_3OH) were purchased from SDS and were dried as necessary by conventional techniques.[30] General synthetic reagents were purchased from Sigma–Aldrich, Fluka, Merck, or SDS, and were used as received. Fmoc-Phe-OH and Fmoc-Leu-OH were acquired from Iris Biotech; benzotriazol-1-yl-oxytris(pyrrolidino)phosphonium hexafluorophosphate (PyBOP), 1-hydroxy-7-azabenzotriazole (HOAt), and *N*-cyclohexylcarbodiimide-*N*′-methyl polystyrene HL were purchased from Novabiochem; the 2-chlorotrityl resin was purchased from CBL Patras. Reactions run under anhydrous conditions were performed in flame-dried glassware, by means of septum and syringe techniques, under an atmosphere of purified N_2.

Synthesis of (R)-N-Boc-3-amino-3-aryl vinyl sulfones 1–5

Representative procedure: synthesis of (3*R*,*E*)-3-(*tert*-butoxycarbonylamino)-3-(2-naphthyl)-1-phenylsulfonyl-1-propene (3): D-(−)-DIPT (90 mg, 0.40 mmol), $Ti(OiPr)_4$ (60 μL, 0.20 mmol), and *t*BuOOH (4.0 mL of a 2 M solution in isooctane; 8.0 mmol) were added sequentially to a cold (−20 °C), stirred suspension of 4 Å powdered molecular sieves (previously activated, 120 mg) in anhydrous CH_2Cl_2 (4 mL) under N_2 atmosphere. After stirring 1 h at −20 °C, a solution of (2*E*)-3-(2-naphthyl)-2-propen-1-ol[31] (0.70 g, 4.0 mmol) in anhydrous CH_2Cl_2 (2 mL) was added via syringe. After stirring for 3 h at the same temperature, the reaction mixture was treated with an aqueous NaOH solution (0.8 mL, 10% in brine) and diluted with Et_2O (9 mL). The temperature was then raised to 10 °C, and anhydrous $MgSO_4$ (0.8 g) and Celite (0.1 g) were added. After stirring for 15 min, the resulting mixture was filtered through Celite, washed with Et_2O, and the solvents were removed under reduced pressure. The crude product was purified by chromatography (silica gel column, hexanes/EtOAc mixtures of increasing polarity) to afford (2*S*,3*R*)-2,3-epoxy-3-(2-naphthyl)propanol (0.52 g, 68% yield) with a 98:2 er (Mosher's ester).

A mixture of this epoxy alcohol (3.1 g, 15.5 mmol), $LiClO_4$ (41.2 g, 0.39 mol), and NaN_3 (5.0 g, 78 mmol) in dry CH_3CN (75 mL) was stirred at 65 °C for 3 h. After cooling to room temperature, the reaction mixture was poured over H_2O (950 mL) and extracted thoroughly with Et_2O. After drying the mixture over $MgSO_4$, evaporation of the solvents afforded 3.6 g (96% yield) of (2*S*,3*S*)-3-azido-3-(2-naphthyl)propane-1,2-diol. Without further purification, this compound (3.4 g, 14 mmol) was dissolved in EtOAc (36 mL) and hydrogenated at atmospheric pressure (balloon) using 10% Pd/C as a catalyst (0.34 g) in the presence of di-*tert*-butyl dicarbonate (4.0 g, 18 mmol). After stirring the compound for 27 h at room temperature and filtering over Celite, evaporation of the solvents was followed by chromatographic purification (silica gel column, hexanes/EtOAc mixtures of increasing polarity) to give 2.7 g (61% yield) of (2*S*,3*S*)-3-(*tert*-butoxycarbonylamino)-3-(2-naphthyl)propane-1,2-diol.

A solution of the above diol (2.5 g, 8.0 mmol), PPh_3 (2.3 g, 8.6 mmol) and diisopropyl azodicarboxylate (1.7 mL, 8.6 mmol) in anhydrous $CHCl_3$ (42 mL) was heated at reflux for 4.5 h. After cooling to room temperature, the solvent was eliminated under reduced pressure and the residue subjected to column chromatography (silica gel, hexanes/EtOAc mixtures of increasing polarity) to afford 2.0 g (84% yield) of (*S*)-2-[(*S*)-1-(*tert*-butoxycarbonylamino)-1-(2-naphthyl)methyl]oxirane. A solution of this oxirane (0.90 g, 3.0 mmol), Et_3N (0.43 mL, 3.0 mmol) and PhSH (0.31 mL, 3.0 mmol) in anhydrous CH_3OH (30 mL), under a N_2 atmosphere, was heated at reflux for 1 h. Evaporation of the solvent under reduced pressure gave 1.3 g (quantitative yield) of (2*S*,3*S*)-3-(*tert*-butoxycarbonylamino)-3-(2-naphthyl)-1-phenylthio-2-propanol. Without further purification, this compound (3.0 mmol) was dissolved in dry CH_2Cl_2 (60 mL), and a solution of purified *m*-chloroperbenzoic acid (1.30 g, 7.5 mmol) was added dropwise. After stirring the solution for 1.5 h at room temperature, excess peroxy acid was destroyed by washing with 10% aqueous Na_2SO_3. The organic phase was washed with aqueous saturated $NaHCO_3$ and brine then dried over $MgSO_4$. The solvent was removed by rotary evaporation. Purification of the crude product by column chromatography (Et_3N-pretreated silica gel, hexanes/EtOAc mixtures of increasing polarity) to afford 0.93 g (70% yield) of (2*S*,3*S*)-3-(*tert*-butoxycarbonylamino)-3-(2-naphthyl)-1-phenylsulfonyl-2-propanol.

A solution of the above hydroxysulfone (0.70 g, 1.6 mmol), morpholinocarbonyldiimidazole (morpho-CDI, 1.35 g, 3.2 mmol) and anhydrous $CuCl_2$ (22 mg, 0.16 mmol) in anhydrous CH_3CN (40 mL) was stirred at 70 °C for 30 min. After cooling to room temperature, the reaction mixture was filtered through Celite to give, upon removal of the solvent, 0.69 g (quantitative yield) of (3*R*,*E*)-3-(*tert*-butoxycarbonylamino)-3-(2-naphthyl)-1-phenylsulfonyl-1-propene (**3**).

(3*R*,*E*)-3-(*tert*-Butoxycarbonylamino)-3-phenyl-1-phenylsulfonyl-1-propene (1): See ref. [26] for spectral data for this compound.

(3*R*,*E*)-3-(*tert*-Butoxycarbonylamino)-3-(1-naphthyl)-1-phenylsulfonyl-1-propene (2): See the Supporting Information.

(3*R*,*E*)-3-(*tert*-Butoxycarbonylamino)-3-(2-naphthyl)-1-phenylsulfonyl-1-propene (3): Colorless solid, mp: 150–152 °C; $[\alpha]_D = +45.1$ ($c = 1.4$, acetone); ^1H NMR (200 MHz, $CDCl_3$): $\delta = 1.39$ (s, 9H), 4.95 (br, 1H), 5.64 (br m, 1H), 6.55 (dd, $J = 15.0$ Hz, $J' = 1.8$ Hz, 1H), 7.21

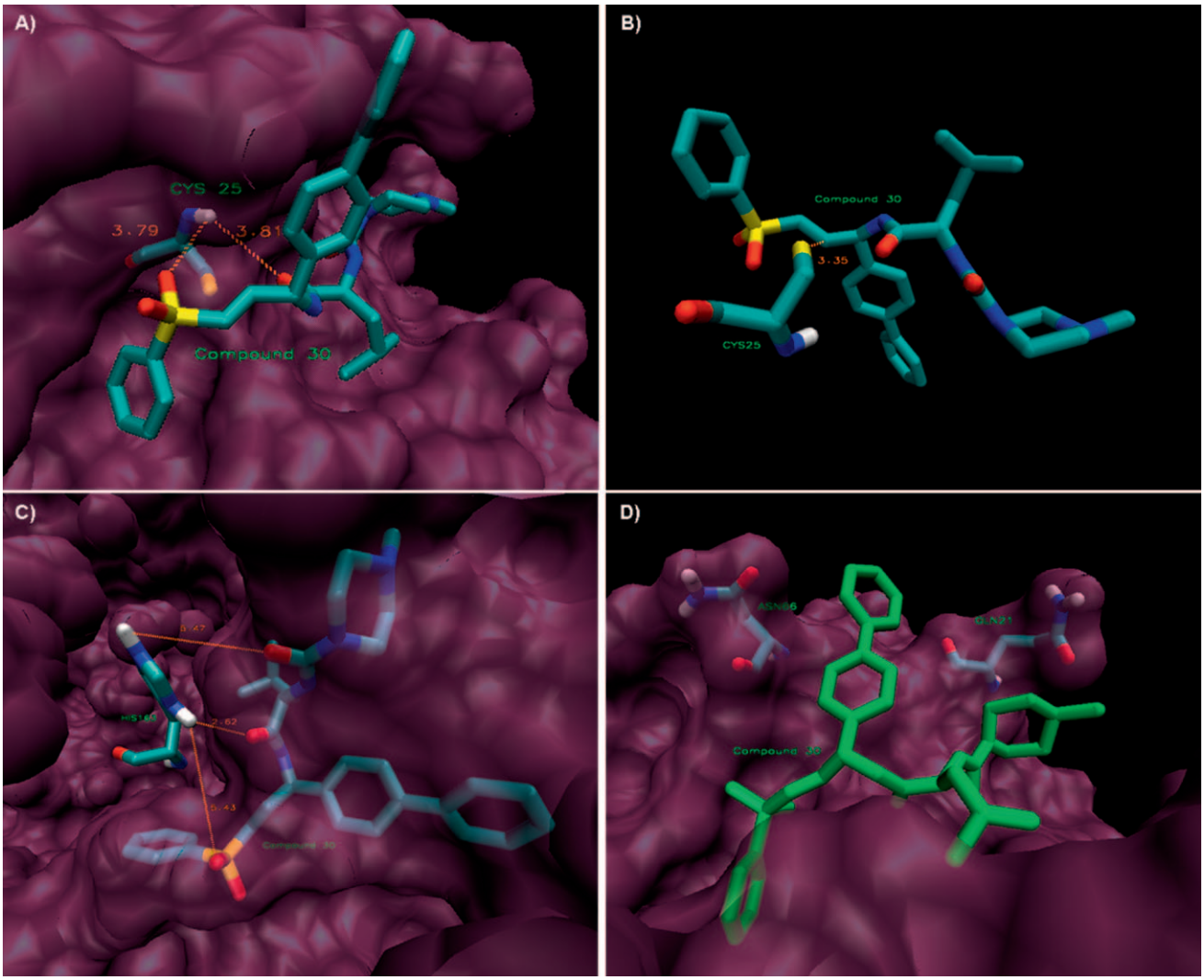

Figure 5. Docking images of compound **30** with cathepsin L. A) Interaction between Cys25 and compound **30**. B) Interaction between the sulfur atom of the active site cysteine and compound **30**. C) Interaction between the active site histidine and compound **30**. D) Cleft defined by Asn66 and Gln21 into which the 4′-biphenyl substituent projects.

(dd, $J=15.0$ Hz, $J'=4.8$ Hz, 1H), 7.32 (dd, $J=8.4$ Hz, $J'=1.8$ Hz, 1H), 7.52–7.64 (m, 6H), 7.82–7.90 ppm (m, 5H); ^{13}C NMR (50 MHz, $CDCl_3$): $\delta=28.2$ (CH_3), 55.1 (CH), 80.5 (C), 124.7, 126.2, 126.6, 126.7, 127.6, 127.9, 129.2, 129.3, 131.3 (CH), 133.0, 133.2 (C), 133.4 (CH), 135.2, 140.0 (C), 145.2 (CH), 154.5 ppm (C); MS (CI, NH_3): $m/z=441$ ([M+18], 77%), 385 ([M−38], 100%).

(3*R*,*E*)-3-(*tert*-Butoxycarbonylamino)-3-(2,4,6-trimethylphenyl)-1-phenylsulfonyl-1-propene (4): See the Supporting Information.

(3*R*,*E*)-3-(*tert*-Butoxycarbonylamino)-3-(4′-biphenyl)-1-phenylsulfonyl-1-propene (5): See the Supporting Information.

Synthesis of (*R*)-3-Amino-3-aryl vinyl sulfone trifluoroacetate salts 6–10: A solution of the *N*-Boc amino vinyl sulfone **1–5** (500 μmol) in 40% TFA in CH_2Cl_2 (1 mL) was stirred at room temperature for 30 min. The solvent and excess TFA were removed under a stream of N_2, and the resulting product was lyophilized and characterized by ^{1}H NMR spectroscopy.

(3*R*,*E*)-3-Amino-3-phenyl-1-phenylsulfonyl-1-propene trifluoroacetate salt (6): See the Supporting Information.

(3*R*,*E*)-3-Amino-3-(1-naphthyl)-1-phenylsulfonyl-1-propene trifluoroacetate salt (7): See the Supporting Information.

(3*R*,*E*)-3-Amino-3-(2-naphthyl)-1-phenylsulfonyl-1-propene trifluoroacetate salt (8): ^{1}H NMR (400 MHz, CD_3OD): $\delta=5.42$ (d, $J=$ 6.4 Hz, 1H), 6.95 (dd, $J=15.2$ Hz, $J'=1.2$ Hz, 1H), 7.22 (dd, $J=$ 15.2 Hz, $J'=6.4$ Hz, 1H), 7.45 (dd, $J=8.4$ Hz, $J'=1.8$ Hz, 1H), 7.55–7.63 (m, 4H), 7.71 (m, 1H), 7.87–7.91 (m, 5H), 7.98 ppm (d, $J=$ 8.4 Hz, 1H).

(3*R*,*E*)-3-Amino-3-(2,4,6-trimethylphenyl)-1-phenylsulfonyl-1-propene trifluoroacetate salt (9): See the Supporting Information.

(3*R*,*E*)-3-Amino-3-(4′-biphenyl)-1-phenylsulfonyl-1-propene trifluoroacetate salt (10): See the Supporting Information.

Incorporation of Fmoc-amino acids to the chlorotrityl chloride resin: The resin (1.0 g, functionalization 1.54 mmol g^{-1}) was conditioned with CH_2Cl_2 and subsequently treated with the Fmoc-amino acid (0.7 equiv) in the presence of DiPEA (1.8 mL, 110 mmol, 7.0 equiv) for 1 h at room temperature. The resin was then treated with CH_3OH (10 min at room temperature) and washed with CH_2Cl_2. Removal of the Fmoc group was effected by treatment with DMF (5×1 min), 20% piperidine in DMF (2×10 min), and DMF (5×1 min). Final functionalization was determined by spectrophotometric analysis of the piperidine–dibenzofulvene adduct in solu-

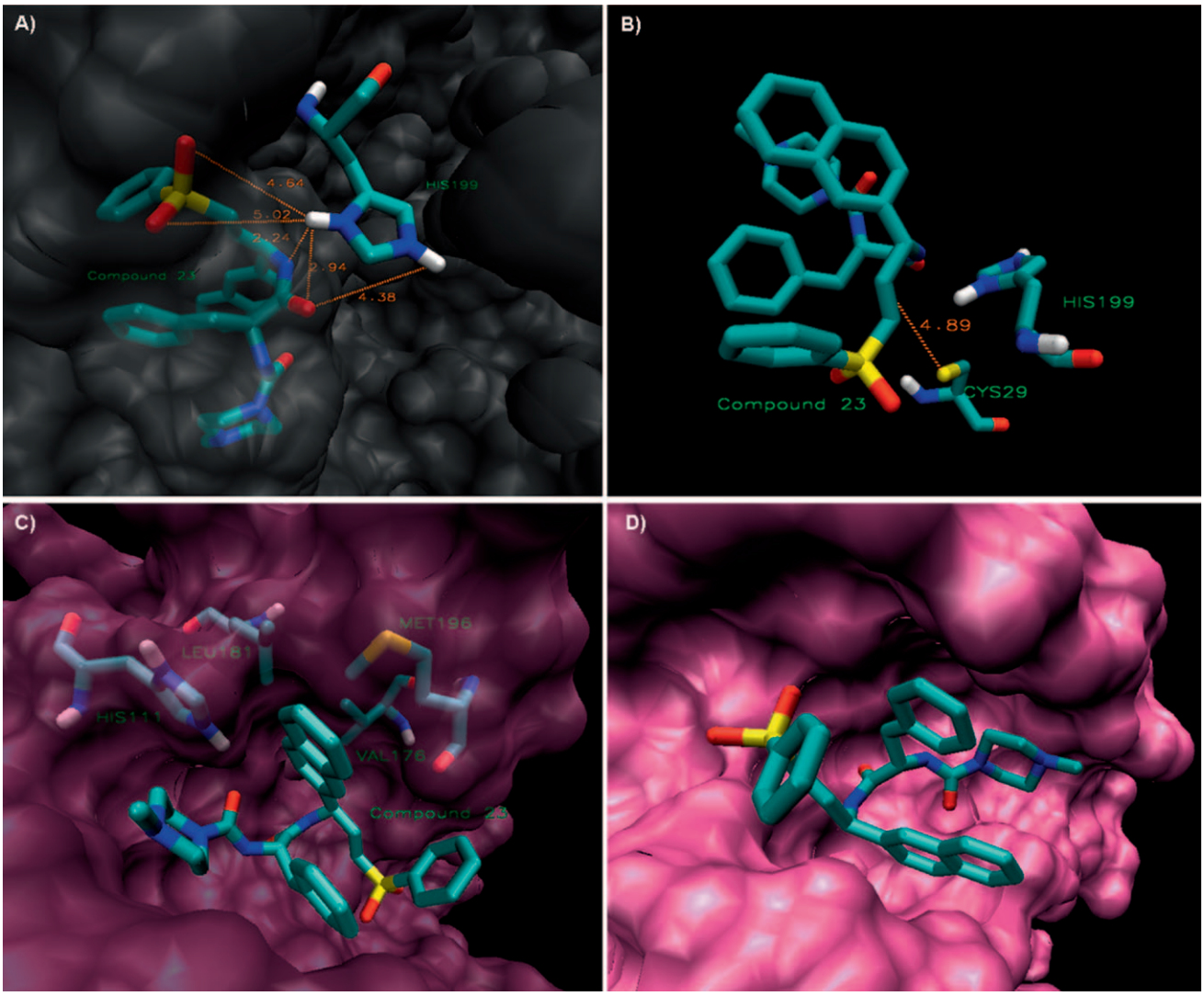

Figure 6. Docking images of compound **23** and cathepsin B. A) Interaction between the active site cysteine and compound **23**. B) Interactions between His199 and compound **23**. C) Amino acid environment of the 2-naphthyl group. D) Compound **23** docked into the active site of cathepsin B.

tion (Fmoc-Phe-OH: functionalization 0.884 mmol g^{-1}, 82% yield; Fmoc-Leu-OH: functionalization 0.892 mmol g^{-1}, 83% yield).

Synthesis of morpholineurea conjugates: The resin-bound amino acid obtained above (1.0 g each) was conditioned with DMF and treated with 4-morpholinocarbonyl chloride (230 μL, 2.0 mmol) and with Hünig's base (510 μL, 3.0 mmol) for 16 h at room temperature. The coupling was controlled by the Kaiser test (ninhydrin), and the urea–amino acid conjugate was cleaved from the resin by treatment with 2% TFA in CH_2Cl_2 (3×10 min). The resin was washed with CH_2Cl_2 and the resulting solution concentrated by a stream of N_2 prior to lyophilization. The crude product was analyzed by HPLC (Symmetry C_{18} column, 5 μm, 4.6×150 mm, $\Phi = 1$ mL min^{-1}, $H_2O \rightarrow$ 0.045% TFA/$CH_3CN \rightarrow$0.036% TFA, gradient from 0 to 100% in 15 min, 25 °C) and by HPLC–MS, and purified by preparative HPLC (Symmetry C_{18} column, 5 μm, 100×30 mm, $\Phi = 10$ mL min^{-1}, $H_2O \rightarrow$0.1% TFA/$CH_3CN \rightarrow$0.05% TFA).

Morpholineurea–phenylalanine conjugate, Mu-Phe-OH: 195 mg of a colorless solid, 79% yield; $t_R = 6.41$ min; MS (ESP+): $m/z = 279.4$ $[M+1]^+$.

Morpholineurea–leucine conjugate, Mu-Leu-OH: 180 mg of a colorless solid, 83% yield. $t_R = 6.11$ min; MS (ESP+): $m/z = 245.4$ $[M+1]^+$.

Synthesis of the *N*-methylpiperazineurea conjugates: The resin-bound amino acid (1.0 g each) was conditioned with DMF and treated with carbonyl diimidazole (810 mg, 5.0 mmol) for 3 h at room temperature. After filtration and washing of the resin with DMF, *N*-methylpiperazine (2.2 mL, 20 mmol) was added; stirring in DMF was maintained for 1 h at room temperature. The coupling was controlled by the Kaiser test (ninhydrin), and the urea–amino acid conjugate was cleaved from the resin by treatment with 2% TFA in CH_2Cl_2 (3×10 min). The resin was washed with CH_2Cl_2 and the resulting solution concentrated by a stream of N_2 prior to lyophilization. The crude product was analyzed by HPLC (Symmetry C_{18} column, 5 μm, 4.6×150 mm, $\Phi = 1$ mL min^{-1}, $H_2O \rightarrow$0.045% TFA/$CH_3CN \rightarrow$0.036% TFA, gradient from 0 to 100% in 15 min, 25 °C) and by HPLC–MS, and purified by preparative HPLC (Symmetry C_{18} column, 5 μm, 100×30 mm, $\Phi = 10$ mL min^{-1}, $H_2O \rightarrow$0.1% TFA/$CH_3CN \rightarrow$0.05% TFA).

***N*-Methylpiperazineurea–phenylalanine conjugate, Npipu-Phe-OH:** 290 mg of a colorless solid, 100% yield; $t_R = 5.02$ min; ^{1}H NMR

(400 MHz, [D_6]DMSO + [D]TFA): δ = 2.80 (s, 3H), 2.88–3.00 (m, 5H), 3.09 (dd, J = 13.6 Hz, J' = 4.4 Hz, 1H), 3.37–3.41 (m, 2H), 4.03–4.11 (m, 2H), 4.29 (dd, J = 10.4 Hz, J' = 4.4 Hz, 1H), 7.20–7.28 ppm (m, 5H); ^{13}C NMR (100 MHz, [D_6]DMSO + [D]TFA): δ = 37.3 (CH_2), 41.5 (CH_2), 42.8 (CH_3), 52.8 (CH_2), 56.1 (CH), 126.9 (CH), 128.7 (CH), 129.8 (CH), 138.9 (C), 157.4 (C), 174.6 ppm (C); MS (MALDI): m/z = 292.1 $[M+1]^+$, 314.1 $[M+23]^+$, 330.1 $[M+39]^+$.

_N_-methylpiperazineurea–leucine conjugate, Npipu-Leu-OH: 140 mg of a colorless solid, 61% yield. t_R = 4.65 min; ^{1}H NMR (400 MHz, [D_6]DMSO + [D]TFA): δ = 0.83 (d, J = 6.4 Hz, 3H), 0.88 (d, J = 6.4 Hz, 3H), 1.44–1.67 (m. 3H), 2.81 (s, 3H), 2.93–3.06 (m, 4H), 3.41 (br d, 2H), 4.06–4.16 ppm (m, 3H); ^{13}C NMR (100 MHz, [D_6]DMSO + [D]TFA): δ = 21.7 (CH_3), 23.4 (CH_3), 25.0 (CH), 41.5 (CH_2), 42.7 (CH_3), 52.6 (CH), 52.9 (CH_2), 157.6 (C), 175.7 ppm (C); MS (MALDI): m/z = 258.1 $[M+1]^+$.

Solution-phase coupling: construction of the peptidyl 3-aryl vinyl sulfone library

Method A (PyBOP): PyBOP (28.6 mg, 55 μmol), HOAt (15 mg, 110 μmol) and DiPEA (9.4 mL, 55 μmol) were added sequentially to a magnetically stirred solution of the urea–amino acid conjugate (55 μmol) in dry CH_2Cl_2 (3 mL). After stirring for 5 min at room temperature, the amino vinyl sulfone salt **5**–**10**(50 μmol) was added, followed by an equimolar amount of DiPEA (8.5 μL, 50 μmol). The resulting mixture was stirred for 30 min, then the solvent was removed by a stream of N_2 and the residue was lyophilized. The crude product was analyzed by HPLC (Symmetry C_{18} column, 5 μm, 4.6×150 mm, Φ = 1 mL min^{-1}, H_2O→0.045% TFA/CH_3CN→0.036% TFA, gradient from 0 to 100% in 15 min, 25 °C) and by HPLC–MS, and purified by preparative HPLC (Symmetry C_{18} column, 5 μm, 100×30 mm, Φ = 10 mL min^{-1}, H_2O→0.1% TFA/CH_3CN→0.05% TFA).

Method B (DCCI resin): *N*-Cyclohexylcarbodiimide-*N*′-methyl polystyrene HL resin (80 mg, functionalization 1.9 mmol g^{-1}, 150 μmol) and Hünig's base (9.4 mL, 55 μmol) were added sequentially to a magnetically stirred solution of the urea–amino acid conjugate (55 μmol) in dry CH_2Cl_2 (3 mL). After stirring for 5 min at room temperature, the amino vinyl sulfone salt (**5**–**10**; 50 μmol) was added, followed by an equimolar amount of DiPEA base (8.5 μL, 50 μmol). The resulting mixture was stirred for 30 min, the solvent was removed by a stream of N_2 and the residue lyophilized. The crude product was analyzed by HPLC (Symmetry C_{18} column, 5 μm, 4.6×150 mm, Φ = 1 mL min^{-1}, H_2O→0.045% TFA/CH_3CN→0.036% TFA, gradient from 0 to 100% in 15 min, 25 °C) and by HPLC–MS, and purified by preparative HPLC (Symmetry C_{18} column, 5 μm, 100×30 mm, Φ = 10 mL min^{-1}, H_2O→0.1% TFA/CH_3CN→0.05% TFA).

***N*-((*S*)-1-Oxo-3-phenyl-1-((*R*,*E*)-1-phenyl-3-(phenylsulfonyl)allylamino)propan-2-yl)morpholine-4-carboxamide (11):** See the Supporting Information.

***N*-((*S*)-1-((*R*,*E*)-1-(Naphthalen-1-yl)-3-(phenylsulfonyl)allylamino)-1-oxo-3-phenylpropan-2-yl)morpholine-4-carboxamide (12):** See the Supporting Information.

***N*-((*S*)-1-((*R*,*E*)-1-(Naphthalen-2-yl)-3-(phenylsulfonyl)allylamino)-1-oxo-3-phenylpropan-2-yl)morpholine-4-carboxamide (13):** **Method A:** Colorless solid (3.0 mg, yield 6%); ^{1}H NMR (400 MHz, $CDCl_3$): δ = 3.06 (m, 2H, CH_2Ph), 3.21 (m, 4H, $2CH_2N$), 3.55 (m, 4H, $2CH_2O$), 4.57 (m, 1H, CHN), 5.05 (br d,1H, NH), 5.85 (m, 1H, CHN-2Nph), 6.20 (dd, J = 15.2 Hz, J' = 1.8 Hz, 1H, =CHS), 6.83 (br d, 1H, NH), 7.04 (dd, J = 15.2 Hz, J' = 4.8 Hz, 1H, CH=), 7.14–7.27 (m, 7H, H_{ar}), 7.47–7.88 ppm (m, 10H, H_{ar}); ^{13}C NMR (100 MHz, $CDCl_3$): δ = 38.5 (CH_2, CH_2Ph), 43.9 (CH_2, CH_2N), 53.5 (CH, 2NphCHN), 56.0 (CH, CHN), 66.2 (CH_2, CH_2O), 124.6, 126.3, 126.7, 126.8, 127.4, 127.7, 127.8, 127.9, 129.0, 129.2, 129.3 (CH, CH_{ar}), 131.6 (CH, =CHS), 133.0, 133.2 (C, C_{ar}), 133.6 (CH, CH_{ar}), 134.7, 136.5, 140.1 (C, C_{ar}), 144.2 (CH, CH=), 157.0 (C, C=O-urea), 171.3 ppm (C, C=O); MS (MALDI): m/z = 584.2 $[M+1]^+$, 606.2 $[M+23]^+$, 622.2 $[M+39]^+$; HPLC t_R = 10.55 min (gradient 0→100% CH_3CN in 15 min).

(*S*)-*N*-((*R*,*E*)-1-(2,4,6-Trimethylphenyl)-3-(phenylsulfonyl)allyl)-2-morpholino-3-phenylpropanamide (14): See the Supporting Information.

***N*-((*S*)-1-((*R*,*E*)-1-(Biphenyl-4-yl)-3-(phenylsulfonyl)allylamino)-1-oxo-3-phenylpropan-2-yl)morpholine-4-carboxamide (15):** See the Supporting Information.

***N*-((*S*)-4-Methyl-1-oxo-1-((*R*,*E*)-1-phenyl-3-(phenylsulfonyl)allylamino)pentan-2-yl)morpholine-4-carboxamide (16):** See the Supporting Information.

***N*-((*S*)-4-Methyl-1-((*R*,*E*)-1-(naphthalen-1-yl)-3-(phenylsulfonyl)allylamino)-1-oxopentan-2-yl)morpholine-4-carboxamide (17):** See the Supporting Information.

***N*-((*S*)-4-Methyl-1-((*R*,*E*)-1-(naphthalen-2-yl)-3-(phenylsulfonyl)allylamino)-1-oxopentan-2-yl)morpholine-4-carboxamide (18):** **Method A:** Colorless solid (8.0 mg, yield 16%); ^{1}H NMR (400 MHz, $CDCl_3$): δ = 0.89 (d, J = 6.4 Hz, 3H, $CH(CH_3)_2$), 0.92 (d, J = 6.4 Hz, 3H, $CH(CH_3)_2$), 1.50–1.64 (m, 3H, $CH_2CH(CH_3)_2$), 3.21 (m, 4H, $2CH_2N$), 3.53 (m, 4H, $2CH_2O$), 4.00 (br s, 1H, NH), 4.44 (m, 1H, NH), 5.08 (br s, 1H, NH), 5.88 (m, 1H, 2-NphCHN), 6.50 (dd, J = 15.0 Hz, J' = 2.0 Hz, 1H, =CHS), 7.17 (dd, J = 15.0 Hz, J' = 5.2 Hz, 1H, CH=), 7.22 (dd, J = 8.4 Hz, J' = 2.0 Hz, H_{ar}), 7.47–7.88 ppm (m, 11H, H_{ar}); ^{13}C NMR (100 MHz, $CDCl_3$): δ = 22.2 (CH_3, $CH(CH_3)_2$), 22.8 (CH_3, $CH(CH_3)_2$), 24.9 (CH, $CH(CH_3)_2$), 40.8 (CH_2, CH_2CH), 43.9 (CH_2, CH_2N), 53.0 (CH, CHN), 53.6 (CH, 2-NphCHN), 66.1 (CH_2, CH_2O), 124.6, 126.3, 126.7, 127.6, 127.7, 128.0, 129.1, 129.4, 129.5 (CH, CH_{ar}), 131.9 (CH, =CHS), 133.0, 133.2 (C, C_{ar}), 133.6 (CH, CH_{ar}), 134.5, 140.0 (C, C_{ar}), 144.3 (CH, CH=), 157.4 (C, C=O-urea), 173.2 ppm (C, C=O); MS (MALDI): m/z = 550.2 $[M+1]^+$, 572.2 $[M+23]^+$, 588.2 $[M+39]^+$; HPLC t_R = 10.47 min (gradient 0→100% CH_3CN in 15 min).

(*S*)-*N*-((*R*,*E*)-1-(2,4,6-Trimethylphenyl)-3-(phenylsulfonyl)allyl)-4-methyl-2-morpholinopentanamide (19): See the Supporting Information.

***N*-((*S*)-1-((*R*,*E*)-1-(Biphenyl-4-yl)-3-(phenylsulfonyl)allylamino)-4-methyl-1-oxopentan-2-yl)morpholine-4-carboxamide (20):** See the Supporting Information.

4-Methyl-*N*-((*S*)-1-oxo-3-phenyl-1-((*R*,*E*)-1-phenyl-3-(phenylsulfonyl)allylamino)propan-2-yl)piperazine-1-carboxamide (21): See the Supporting Information.

4-Methyl-*N*-((*S*)-1-((*R*,*E*)-1-(naphthalen-1-yl)-3-(phenylsulfonyl)allylamino)-1-oxo-3-phenylpropan-2-yl)piperazine-1-carboxamide (22): See the Supporting Information.

4-Methyl-*N*-((*S*)-1-((*R*,*E*)-1-(naphthalen-2-yl)-3-(phenylsulfonyl)allylamino)-1-oxo-3-phenylpropan-2-yl)piperazine-1-carboxamide (23): **Method B:** Colorless solid (18.2 mg, yield 61%); ^{1}H NMR (400 MHz, $CDCl_3$): δ = 2.28 (br, 2H, CH_2N), 2.43 (s, 3H, CH_3N), 3.03 (m, 2H, CH_2Ph), 3.10 (br, 4H, $2CH_2N$), 3.79 (br, 2H, CH_2N), 4.58 (m, 1H, CHN), 5.83 (m, 1H, CHN-2Nph), 6.17 (br d, 1H, NH), 6.21 (dd, J = 15.0 Hz, J' = 2.4 Hz, 1H, =CHS), 7.03 (dd, J = 15.0 Hz, J' = 4.8 Hz, 1H, CH=), 7.15–7.20 (m, 6H, H_{ar}), 7.41–7.80 ppm (m, 12H, 11H_{ar}, NH); ^{13}C NMR (100 MHz, $CDCl_3$): δ = 38.5 (CH_3, CH_2Ph), 41.0 (CH_2, CH_2N), 43.0 (CH_3, CH_3N), 52.6 (CH_2, CH_2N), 53.5 (CH, CHN-2Nph), 56.7 (CH, CHN), 124.6, 126.1, 126.7, 127.2, 127.6, 127.7, 127.9, 128.7, 129.1, 129.2, 129.4 (CH, CH_{ar}), 131.5 (CH, =CHS), 132.8, 133.1 (C, C_{ar}), 133.7 (CH, CH_{ar}), 135.0, 136.6, 139.7 (C, C_{ar}), 144.7 (CH, CH=), 156.5 (C, C=O-urea), 172.2 ppm (C, C=O); MS (MALDI): m/z = 597.2 $[M+1]^+$, 619.2 $[M+23]^+$, 635.2 $[M+39]^+$; HPLC t_R = 9.02 min (gradient 0→100% CH_3CN in 15 min).

(*S*)-*N*-((*R*,*E*)-1-(2,4,6-Trimethylphenyl)-3-(phenylsulfonyl)allyl)-2-(4-methylpiperazin-1-yl)-3-phenylpropanamide (24): See the Supporting Information.
N-((*S*)-1-((*R*,*E*)-1-(Biphenyl-4-yl)-3-(phenylsulfonyl)allylamino)-1-oxo-3-phenylpropan-2-yl)-4-methylpiperazine-1-carboxamide (25): See the Supporting Information.
4-Methyl-*N*-((*S*)-4-methyl-1-oxo-1-((*R*,*E*)-1-phenyl-3-(phenylsulfonyl)allylamino)pentan-2-yl)piperazine-1-carboxamide (26): See the Supporting Information.
4-Methyl-*N*-((*S*)-4-methyl-1-((*R*,*E*)-1-(naphthalen-1-yl)-3-(phenylsulfonyl)allylamino)-1-oxopentan-2-yl)piperazine-1-carboxamide (27): See the Supporting Information.
4-Methyl-*N*-((*S*)-4-methyl-1-((*R*,*E*)-1-(naphthalen-2-yl)-3-(phenylsulfonyl)allylamino)-1-oxopentan-2-yl)piperazine-1-carboxamide (28): Method B: Colorless solid (16.0 mg, yield 57%); ^{1}H NMR (400 MHz, $CDCl_3$): $\delta = 0.80$ (d, $J = 6.0$ Hz, 3H, $CH(CH_3)_2$), 0.83 (d, $J = 6.0$ Hz, 3H, $CH(CH_3)_2$), 1.50–1.59 (m, 3H, $CH_2CH(CH_3)_2$), 2.48 (br, 2H, CH_2N), 2.53 (s, 3H, CH_3N), 3.18 (br, 4H, $2CH_2N$), 3.99 (br, 2H, CH_2N), 4.32 (m, 1H, CHN), 5.93 (m, 1H, CHN-2Nph), 6.25 (br d, 1H, NH), 6.57 (dd, $J = 15.2$ Hz, $J' = 2.0$ Hz, 1H, =CHS), 7.16 (dd, $J = 15.2$ Hz, $J' = 4.8$ Hz, 1H, =CH), 7.24 (dd, $J = 8.4$ Hz, $J' = 1.6$ Hz, 1H, H_{ar}-2Nph), 7.38–7.52 (m, 4H, H_{ar}), 7.59–7.72 (m, 4H, H_{ar}), 7.79–7.81 (m, 2H, H_{ar}), 8.13 ppm (d, $J = 8.4$ Hz, 1H, H_{ar}-2Nph); ^{13}C NMR (100 MHz, $CDCl_3$): $\delta = 21.9$ (CH_3, $CH(CH_3)_2$), 22.7 (CH_3, $CH(CH_3)_2$), 24.8 (CH, $CH(CH_3)_2$), 40.7 (CH_2, $CH_2CH(CH_3)_2$), 41.0 (CH_2, CH_2N), 43.1 (CH_3, CH_3N), 52.9 (CH_2, CH_2N), 53.3 (CH, CHN-2Nph), 54.3 (CH, CHN), 124.8, 126.2, 126.7, 127.5, 127.6, 127.9, 129.0, 129.4 (CH, CH_{ar}), 131.6 (CH, =CHS), 132.8, 133.1 (C, C_{ar}), 133.8 (CH, CH_{ar}), 135.0, 139.6 (C, C_{ar}), 145.0 (CH, CH=), 156.9 (C, C=O-urea), 173.7 ppm (C, C=O); MS (MALDI): $m/z = 563.2$ $[M+1]^+$, 585.2 $[M+23]^+$, 601.2 $[M+39]^+$; HPLC $t_R = 8.95$ min (gradient 0→100% CH_3CN in 15 min).
(*S*)-*N*-((*R*,*E*)-1-(2,4,6-Trimethylphenyl)-3-(phenylsulfonyl)allyl)-4-methyl-2-(4-methylpiperazin-1-yl)pentanamide (29): See the Supporting Information.
N-((*S*)-1-((*R*,*E*)-1-(Biphenyl-4-yl)-3-(phenylsulfonyl)allylamino)-4-methyl-1-oxopentan-2-yl)-4-methylpiperazine-1-carboxamide (30): See the Supporting Information.

Enzyme assays

Cathepsin L (3.4.22.15) and cathepsin B (3.4.22.1), both from human liver, and DPP IV (3.4.14.5) from porcine kidney, were purchased from Sigma–Aldrich (Deisenhofen, Germany). POP was obtained by recombinant expression in *E. coli* as previously described.[32] The cathepsin L substrate used in experiments was Z-Phe-Arg-AMC, the cathepsin B substrate was Z-Arg-Arg-AMC, the POP substrate was Z-Gly-Pro-AMC, and the DPP IV substrate was H-Gly-Pro-AMC. All of them were obtained from Bachem (Bubendorf, Switzerland). NaOAc, Triton X-100, and DTT were purchased from Fluka Chemika (Buchs, Switzerland), EDTA was obtained from USB Corporation (Staufen, Germany), acetic acid was purchased from Carlo Erba Reagenti (Italy), sodium phosphate monobasic and dibasic were acquired from Sigma–Aldrich (Deisenhofen, Germany) and DMSO was provided by Panreac Química S.A.U. (Barcelona, Spain). Fluorescence was measured using a BIO-TEK FL600 Microplate Fluorescence Reader (Bio-Tek Instruments, VT, USA). For inhibition assays, 96-well microplates from Costar (Corning Life Sciences, NY, USA) were used. The cathepsin L buffer was 100 mM NaOAc, containing 0.01% Triton X-100, 5 mM EDTA and 5 mM DTT, with the pH adjusted to 5.5 by the addition of acetic acid. The buffer for cathepsin B was 100 mM sodium phosphate, pH 6.2, 1 mM EDTA and 1 mM DTT. The buffer used for POP and DPP IV was 100 mM sodium/potassium phosphate, pH 8. The cathepsin L enzyme was at a concentration of 70 ng μL^{-1}, cathepsin B enzyme at 6.65 ng μL^{-1}, POP at 10.6 ng μL^{-1}, and DPP IV at 0.187 ng μL^{-1}, with compound stock solutions prepared in DMSO at a final concentration of 5 mM or 25 mM. Dilutions from the stock solution were used in order to perform the inhibition curves.
Cathepsin enzymatic assays were performed at room temperature using 139 μL buffer, 3 μL compound stock solution, 3 μL enzyme, and 5 μL of 3 mM substrate per well. After the addition of buffer, enzyme, and compound, the mixture was pre-incubated for 15 min at 37 °C. Next, the substrate was added, and the mixture was incubated for 30 min at 37 °C. The reaction was stopped by the addition of 150 μL of 1 M NaOAc (pH 4) to each well. The plate was read in the fluorimeter at $\lambda_{excitation} = 360/40$ nm and $\lambda_{emission} = 485/40$ nm.
Time-course experiments were performed at room temperature using 139 μL buffer, 3 μL compound stock solution, 3 μL enzyme, and 5 μL of 3 mM substrate per well. Pre-incubation was done for 0, 5, 10, 15, 30, 60, 90, and 120 min. After pre-incubation, substrate was added, and plates were incubated at 37 °C for 30 min. Following this incubation, the reaction was stopped and fluorescence readings were taken.
POP and DPP IV enzymatic assays were performed at room temperature using 135 μL buffer, 3 μL compound stock solution, 2 μL enzyme, and 10 μL of 3 mM substrate per well. After the addition of buffer, enzyme and compound, the mixture was pre-incubated for 15 min at 37 °C. Next, the substrate was added and the mixture was incubated for 60 min at 37 °C. The reaction was stopped by the addition of 150 μL of 1 M NaOAc (pH 4) to each well. The plate was read in the fluorimeter at $\lambda_{excitation} = 360/40$ nm and $\lambda_{emission} = 485/40$ nm.

Docking

Compounds were drawn using MarvinSketch and translated to three-dimensional viewing with MarvinView. The X-ray crystal structure corresponding to PDB ID: 1CS8 (1.80 Å resolution) was used as the target structure for cathepsin L, with the water molecules, as well as the propeptide sequence, removed from the file. For cathepsin B, the X-ray crystal structure corresponding to PDB ID: 1HUC (2.10 Å resolution) was used, with the water molecules eliminated.
Docking calculations were performed with AutoDock version 4.[33] The protein was set as rigid while the compounds were defined as flexible. A grid map of 60×60×60 points with a point spacing of 0.375 Å (generated using AutoGrid, version 4) was placed in the active center of the enzyme, using AutoDock tools. For each compound, 100 docking runs were carried out using 50 individuals and the Lamarckian genetic algorithm. After calculations, the results were evaluated, and the best docked conformations were selected for further analysis.

Acknowledgements

The authors thank ENANTIA S.L. for their enthusiasm and support of this project. This work was funded by MCYT-FEDER (Bio2008-00799), MEC (AYA2006-15648-C02-01), and the Generalitat de Catalunya (XRB 2009 and Grup Consolidat 2009SGR1005).

Keywords: aryl vinyl sulfones · cathepsins · cysteine proteases · enzymes · medicinal chemistry

[1] D. P. Dickinson, *Crit. Rev. Oral Biol. Med.* **2002**, *13*, 238 – 275.
[2] F. Lecaille, J. Kaleta, D. Brömme, *Chem. Rev.* **2002**, *102*, 4459 – 4488.
[3] R. Vicik, M. Busemann, C. Gelhaus, N. Stiefl, J. Scheiber, W. Schmitz, F. Schulz, M. Mladenovic, B. Engels, M. Leippe, K. Baumann, T. Schirmeister, *ChemMedChem* **2006**, *1*, 1126 – 1141.
[4] M. Söderström, H. Salminen, V. Glumoff, H. Kirschke, H. Aro, E. Vuorio, *Biochim. Biophys. Acta Gene Struct. Expression* **1999**, *1446*, 35 – 46.
[5] R. Xing, A. K. Addington, R. W. Mason, *Biochem. J.* **1998**, *332*, 499 – 505.
[6] C. Palermo, J. A. Joyce, *Trends Pharmacol. Sci.* **2008**, *29*, 22 – 28.
[7] J. A. Joyce, A. Baruch, K. Chehade, N. Meyer-Morse, E. Giraudo, F. Y. Tsai, D. C. Greenbaum, J. H. Hager, M. Bogyo, D. Hanahan, *Cancer Cell* **2004**, *5*, 443 – 453.
[8] J. A. Joyce, D. Hanahan, *Cell Cycle* **2004**, *3*, 1516 – 1519.
[9] M. R. Buck, D. G. Karustis, N. A. Day, K. V. Honn, B. F. Sloane, *Biochem. J.* **1992**, *282*, 273 – 278.
[10] V. Kolkhorst, J. Stürzebecher, B. Wiederanders, *J. Cancer Res. Clin. Oncol.* **1998**, *124*, 598 – 606.
[11] V. Gocheva, W. Zeng, D. Ke, D. Klimstra, T. Reinheckel, C. Peters, D. Hanahan, J. A. Joyce, *Genes Dev.* **2006**, *20*, 543 – 556.
[12] K. M. Bell-McGuinn, A. L. Garfall, M. Bogyo, D. Hanahan, J. A. Joyce, *Cancer Res.* **2007**, *67*, 7378 – 7385.
[13] T. Yasuma, S. Oi, N. Choh, T. Nomura, N. Furuyama, A. Nishimura, Y. Fujisawa, T. Sohda, *J. Med. Chem.* **1998**, *41*, 4301 – 4308.
[14] M. Yamamoto, S. Ikeda, H. Kondo, S. Inoue, *Bioorg. Med. Chem. Lett.* **2002**, *12*, 375 – 378.
[15] J. P. Falgueyret, R. M. Oballa, O. Okamoto, G, Wesolowski, Y. Aubin, R. M. Rydzewski, P. Prasit, D. Riendeau, S. B. Rodan, M. D. Percival, *J. Med. Chem.* **2001**, *44*, 94.
[16] P. D. Greenspan, K. L. Clark, R. A. Tommasi, S. D. Cowen, L. W. McQuire, D. L. Farley, J. H. Van Duzer, R. L. Goldberg, H. Zhou, Z. Du, J. J. Fitt, D. E. Coppa, Z. Fang, W. Macchia, L. Zhu, M. P. Capparelli, R. Goldstein, A. M. Wigg, J. R. Doughty, R. S. Bohacek, A. K. Knap, *J. Med. Chem.* **2001**, *44*, 4524 – 4534.
[17] D. Brömme, J. L. Klaus, K. Okamoto, D. Rasnick, J. T. Palmer, *Biochem. J.* **1996**, *315*, 85 – 89.
[18] J. T. Palmer, D. Rasnick, J. L. Klaus, D. Brömme, *J. Med. Chem.* **1995**, *38*, 3193 – 3196.
[19] E. T. Larson, F. Parussini, M.-H. Huynh, J. D. Giebel, A. M. Kelley, L. Zhang, M. Bogyo, E. A. Merritt, V. B. Carruthers, *J. Biol. Chem.* **2009**, *284*, 26839 – 26850.
[20] J. H. McKerrow, J. C. Engel, C. R. Caffrey, *Bioorg. Med. Chem.* **1999**, *7*, 639 – 644.
[21] J. C. Engel, P. S. Doyle, I. Hsieh, J. H. McKerrow, *J. Exp. Med.* **1998**, *188*, 725 – 734.
[22] T. A. Pauly, T. Sulea, M. Ammirati, J. Sivaraman, D. E. Danley, M. C. Griffor, A. V. Kamath, I. K. Wang, E. R. Laird, A. P. Seddon, R. Ménard, M. Cygler, V. L. Rath, *Biochemistry* **2003**, *42*, 3203 – 3213.
[23] M. E. McGrath, J. L. Klaus, M. G. Barnes, D. Brömme, *Nat. Struct. Biol.* **1997**, *4*, 105 – 109.
[24] J. R. Somoza, J. T. Palmer, J. D. Ho, *J. Mol. Biol.* **2002**, *322*, 559 – 568.
[25] W. Jacobsen, U. Christians, L. Z. Benet, *Drug Metab. Dispos.* **2000**, *28*, 1343 – 1351.
[26] A. Picó, A. Moyano, M. A. Pericàs, *J. Org. Chem.* **2003**, *68*, 5075 – 5083.
[27] R. Ettari, E. Nizi, M. E. Di Francesco, M. A. Dude, G. Pradel, R. Vicík, T. Schirmeister, N. Micale, S. Grasso, M. Zappalà, *J. Med. Chem.* **2008**, *51*, 988 – 996.
[28] M. G. Götz, C. R. Caffrey, E. Hansell, J. H. McKerrow, J. C. Powers, *Bioorg. Med. Chem.* **2004**, *12*, 5203 – 5211.
[29] D. Musil, D. Zucic, D. Turk, R. A. Engh, I. Mayr, R. Huber, T. Popovic, V. Turk, T. Towatari, N. Katunuma, *EMBO J.* **1991**, *10*, 2321 – 2330.
[30] D. D. Perrin, W. L. F. Armarego, *Pergamon Press*, Oxford, **1988**.
[31] T. D. Avery, D. Calazza, J. A. Culbert, D. K. Taylor, R. T. Edward, *J. Org. Chem.* **2005**, *70*, 8344 – 8351.
[32] T. Tarragó, S. Frutos, R. A. Rodríguez-Mias, E. Giralt, *ChemBioChem* **2006**, *7*, 827 – 833.
[33] G. M. Morris, D. S. Goodsell, R. Huey, A. J. Olson, *J. Comput. Aided Mol. Des.* **1996**, *10*, 293 – 304 .

Received: March 17, 2010
Revised: June 8, 2010
Published online on July 22, 2010

